Talanta 117 (2013) 456–462

Contents lists available at ScienceDirect

Talanta

journal homepage: www.elsevier.com/locate/talanta

Simultaneous determination of nanomolar nitrite and nitrate in seawater using reverse flow injection analysis coupled with a long path length liquid waveguide capillary cell

Sichao Feng, Min Zhang, Yongming Huang, Dongxing Yuan*, Yong Zhu

State Key Laboratory of Marine Environmental Science, Environmental Science Research Center, College of the Environment & Ecology, Xiamen University, Xiamen 361102, People's Republic of China

ARTICLE INFO

Article history:
Received 18 June 2013
Received in revised form
20 September 2013
Accepted 22 September 2013
Available online 25 September 2013

Keywords:
Nanomolar nitrite and nitrate
Reverse flow injection analysis
Liquid waveguide capillary cell
Seawater

ABSTRACT

A reverse flow injection analysis (rFIA) method coupled with 1 m liquid waveguide capillary cell and spectrophotometric detection for simultaneous determination of nanomolar nitrite and nitrate in seawater was developed. The design of two analytical channels sharing the same detection system in the proposed method allowed the analysis of both nitrite and nitrate with single sample injection. Different strategies of reagent injection were investigated to obtain a higher sensitivity and a better peak shape. A dual-wavelength detection mode was chosen to eliminate the light source shifting and sample matrix interference. Experimental parameters were optimized based on a univariate experimental design and the matrix effect from seawater was preliminarily investigated. The proposed method had high sensitivity with detection limit of 0.6 nmol L^{-1} for both nitrite and nitrate. The linearity was 2–500 nmol L^{-1} for both analytes, and the upper limit could be extended by choosing a lower sensitivity detection wavelength. The analytical results of 26 surface seawater samples obtained with the proposed method showed good agreement with those using a reference method operated using an automated segmented flow analyzer. The proposed method could greatly minimize the trouble introduced by bubbles in the segmented flow analyzer. It also had the advantages of high precision and high sample throughput (nitrite and nitrate detected in triplicate; 5 h^{-1}). Compared to normal flow injection analysis, the rFIA method is superior due to its lower reagent consumption, less dispersion of sample, as well as higher sensitivity.

1. Introduction

Nitrogen is an essential element for marine phytoplankton growth and plays a crucial role in many biogeochemical cycles [1,2]. Dissolved inorganic nitrogen (DIN) species including nitrite, nitrate and ammonium, as the fixed nitrogen, can be used by many microbes and often limit primary productivity [3]. Nitrite, which is at the intermediate redox position between ammonium and nitrate, concentrates to exceed 50 nmol L^{-1} only within a narrow layer in the ocean, known as the primary nitrite maximum [4]. The distribution of nitrate, which is the principal form of DIN, typically spans up to 5 orders of magnitude in the open ocean, from several nanomolar in surface waters increasing to micromolar with the increase of depth [5]. Accurate quantification of nanomolar nitrite and nitrate is essential for understanding the marine nitrogen cycle and the dynamics of marine ecosystems. However, the conventional spectrophotometric analytical techniques [6,7] which have a detection limit of 100 nmol L^{-1}, are not sensitive enough to detect the variations of nitrite in most open ocean samples and of nitrate in surface water samples.

Much effort has been devoted to the development of new methods for the analysis of nitrite and nitrate at trace level, including chemiluminescence [8–11], fluorescence [12,13] and ion chromatography [14]. However, the methods and instruments in these studies require skilled operators and are mainly lacking in field testing and application, especially compared to the spectrophotometric method. Since it is a challenge to find a new chromogenic agent that has higher selectivity and larger molar absorptivity for nitrite and nitrate [15], the sensitivity-enhanced colorimetric approaches based on the classic Griess assay are still the most popular for the determination of nitrite and nitrate at nanomolar level in seawater. The Griess assay typically relies on the diazotisation of a suitable aromatic amine by reaction of nitrite with sulfanilamide (SAM) and N-1-naphthylethylenediamine dihydrochloride (NED) and the formation of a pink-colored azo dye. Nitrate in the samples is usually reduced to the more-reactive

* Corresponding author. Tel.: +86 592 2184820; fax: +86 592 2180655.
E-mail address: yuandx@xmu.edu.cn (D. Yuan).

0039-9140/$ - see front matter © 2013 Elsevier B.V. All rights reserved.
http://dx.doi.org/10.1016/j.talanta.2013.09.042

nitrite using a copper-coated cadmium column, and then determined through the Griess assay [16].

There are mainly two approaches to enhance the sensitivity of conventional spectrophotometry, one involves enrichment of the azo compound using a solid phase extraction cartridge [17–21] and the other increases the optical path length for the measurement cells by means of liquid waveguide capillary cell (LWCC) devices [15,22–28]. The enrichment method concentrates the chromophore, as well as the reagents, resulting in an increased blank. Therefore this method is sensitive to atmospheric contamination where contaminants gradually dissolve in the reagent, such as in the case of nitrite and nitrate detection. Furthermore, the enrichment method is time consuming and requires large sample volume. According to the Lambert–Beer law, the sensitivity of spectrophotometric methods can be enhanced by extension of the optical path length. The LWCC provides a long optical path length by constraining light propagation within a liquid medium (water) that has a higher refractive index (1.33) than the surrounding solid tubing (1.29) made of a flexible fluoropolymer material (Teflon AF, DuPont) [29]. The LWCC coupled with standard spectrophotometric analysis can simply achieve a very low detection limit and has been widely used for trace element analysis [29,30].

In order to obtain a high sample throughput, high precision and minimum contamination, LWCC is usually combined with automated analytical systems, such as flow injection analysis (FIA), sequential injection analysis (SIA) and segmented continuous flow analysis (SCFA). FIA systems, which have the advantages of higher sample throughput and precision over SIA and can avoid the bubbles introduced in SCFA, have proved to be simple, robust, low-cost and appropriate in nutrient analysis [31]. FIA systems are basically classified into normal FIA (nFIA) and reverse FIA (rFIA). In rFIA, the reagent is injected into a continuously flowing stream of the sample rather than injecting the sample into a continuously flowing carrier solution in nFIA. Based on this, in rFIA the sample dispersion is lessened, analytical sensitivity improved, the matrix effect overcome and consumption of reagent minimized [32]. There is unavoidable contamination from impure reagents or/and carrier solution, which may also have absorbance at the detection wavelength. This interference is sometimes not big enough to be detected in conventional spectrophotometric systems; however in a high sensitive LWCC system, it can cause high background, high noise, and limited linear range. In our experience, if the flow analysis system continually sends the mixture of all reagents and the carrier/sample through the LWCC, the formed compound was absorbed onto the inner wall of the LWCC, leading to attenuation of transmission light. This problem can be eliminated by using rFIA, in which the formed compound only exists in the injected reagent zone, and the sample carrier can behave as a wash solution to keep the LWCC clean. Moreover, since the baseline of the peak obtained in rFIA is the absorbance of the sample solution, the potential interferences from salt effect and colorful compounds in the sample can be corrected using sample absorbance as a background signal.

Recently, simple rFIA systems combined with an LWCC and a spectrophotometric detector have been successfully used for the determination of nanomolar soluble reactive phosphorus and iron in seawater [33,34]. Also, a sensor combined rFIA system and a fluorescence detector has been successfully used for the simultaneous determination of nanomolar concentrations of nitrite, nitrate, and ammonia in seawater [13]. Using the rFIA manifold, the background fluorescence released from dissolved organic matter is corrected for.

There is no reported work relating to the use of an rFIA with an LWCC for simultaneous determination of nanomolar nitrite and nitrate in seawater. In this study, a simple rFIA system coupled with an LWCC was developed for this purpose. Experimental parameters including flow rate, reagent loop, reagent concentration, and length of the mixing coils were investigated to achieve satisfactory sensitivity and precision. The matrix effect was also preliminarily studied.

2. Experimental

2.1. Reagents and solutions

All the chemicals used were of analytical grade, and supplied by Sinopharm Chemical Reagent Co., China (http://www.reagent.com.cn), unless stated otherwise. All solutions were prepared with fresh Milli-Q water (18.20 MΩ cm), obtained from a Millipore Purification Water System (Millipore Co., MA, USA, http://www.millipore.com). All bottles and vials used were soaked in 20% (v/v) HCl for at least 12 h, and rinsed with the Milli-Q water thoroughly.

Nitrite and nitrate stock solution (each 100 mmol L^{-1}) were prepared from solid $NaNO_2$ and KNO_3, which were dried at 105 °C for 1 h. The standard stock solutions were stored at 4 °C in a refrigerator. Working standards were obtained by appropriate dilution of the stock solutions with Milli-Q water daily.

The SAM solution was prepared by dissolving 0.3 g SAM in 200 mL 4% (v/v) HCl (guaranteed grade, Merck, http://www.merck-china.com) solution, and the NED solution was prepared by dissolving 0.03 g NED in 200 mL Milli-Q water. The SAM and NED solutions were prepared daily.

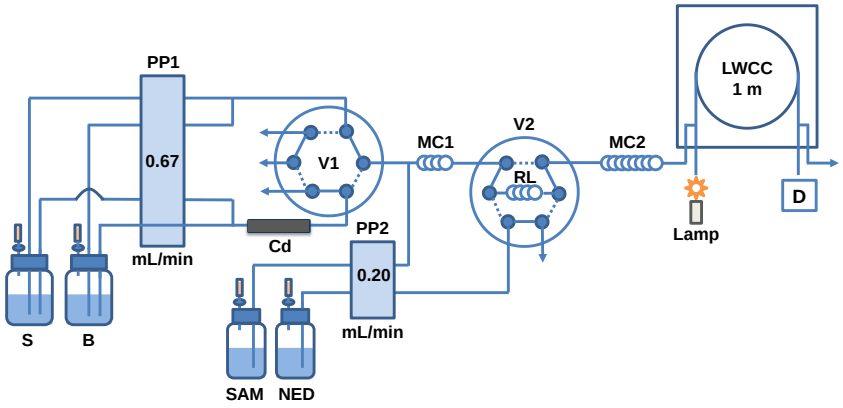

Fig. 1. The rFIA manifold configuration coupled with an LWCC for the determination of nanomolar nitrite and nitrate in seawater. S, sample; B, NH_4Cl buffer solution; PP1 and PP2, peristaltic pumps; V1 and V2, 6-port, 2-position injection valves; Cd, copper-coated cadmium reduction column; MC1 and MC2, mixing coils; RL, reagent loop; D, detector; the solid line of V1 and V2 represents the valve at position A, and the dashed line represents position B.

The NH_4Cl buffer solution was prepared by adding 5.0 g NH_4Cl into 500 mL Milli-Q water, and the pH of solution was adjusted to 8.2 with 50% (v/v) $NH_3 \cdot H_2O$ solution (guaranteed grade).

A column filled with soda lime, with a syringe filter (0.45 μm) at the bottom, was connected to each sample or reagent container to absorb acid gases, e.g. NO_x, and to filter particles from the air, thus allowing clean air to enter the container and so minimize air contamination. Copper-coated cadmium columns were prepared according to the literature [6,35] (details described in the Supplementary material) for reduction of nitrate to nitrite.

Surface seawater samples used for the matrix effect investigation, the recovery test and the intercomparison experiment were collected from the South China Sea in the summer of 2011 and 2012, and stored at −20 °C until analysis.

2.2. Instrumentation and procedures

The rFIA manifold designed is shown in Fig. 1. Two peristaltic pumps, a Lead-1 4-channel peristaltic pump and a BT100-2J 2-channel peristaltic pump (Baoding Longer Precision Pump Co., Hebei, China, http://www.lgpump.com.cn) were used to deliver the sample and reagents. Two 6-port, 2-position injection valves with microelectronic actuators (VICI, Valco Instruments Co., Houston, TX, USA, http://www.vici.com) were adopted for switching analytical channels and injecting the NED solution into the carrier. A 1-m LWCC with 550 μm internal diameter and about 250 μL internal volume (Type-II, World Precision Instruments Inc., Sarasota, FL, USA, http://www.wpiinc.com) was connected to a miniature LS-1-LL tungsten halogen lamp and a miniature multichannel USB 4000 spectrophotometer (Ocean Optics Inc., FL, USA, http://www.oceanoptics.com) via two fiber optic cables.

Silicone tubing was used as the pump tubing. The reagent loop and mixing coils 1 and 2 (MC1 and MC2) were polytetrafluoroethylene (PTFE) tubing of 1.0 mm i.d. and MC2 was made as a knotted reactor. All other tubing for connecting different parts of the manifold was PTFE tubing of 0.75 mm i.d.

Two parallel analytical channels were in the rFIA–LWCC system. One was for nitrite and the other for nitrite+nitrate. The two channels shared the same detection system and were switched by V1. Compared to the method with only one analytical channel, this design did not involve connecting and disconnecting the cadmium column when analyzing nitrate and nitrite, and thus saved analytical time and minimized contamination. When V1 was switched to position A, the sample for determination of nitrite was transported by PP1 and mixed with NH_4Cl buffer solution as a carrier stream, and then the sample–buffer stream was mixed with SAM in MC1. By switching V2 to position A, a constant volume of 160 μL NED solution was injected discretely into the stream. The SAM and NED reacted with nitrite in MC2 to form the pink-colored azo compound, which was delivered through the LWCC for detection. In the nitrite-detection step, the sample for the determination of nitrite+nitrate was continuously transported and merged with the buffer, followed by passing through the cadmium column for nitrate reduction. The time during nitrate detection could be saved for tubing pre-rinsing, which was useful to minimize the carryover effect. With V1 switched to position B, the cadmium column was connected to the analytical manifold. Nitrate in the sample was reduced to nitrite, and nitrite+nitrate was determined as nitrite as described above.

In the LWCC, the azo compound was detected at 540 nm with a background correction at 700 nm. The dual-wavelength spectrophotometric method proved to be simple and effective to compensate for signal fluctuations due to instability of lamp intensity, micro-bubbles within the flow cell, and any Schlieren effect caused by the difference of refractive index between solutions passing through the flow cell, and hence enhancing the signal-to-noise ratio [36]. The concentrations of nitrite and nitrite+nitrate were calculated from the averaged peak height of the output signal using the calibration curve prepared. The nitrate concentration in the sample was obtained by the subtracting nitrite value from the nitrite+nitrate value.

Before and after use, the LWCC was rinsed sequentially with Milli-Q water, 1 mol L^{-1} NaOH (10 mL) and 1 mol L^{-1} HCl (10 mL) solutions and again with Milli-Q water (30 mL) as recommended [29].

For the rFIA with the LWCC in this work, bubbles introduced were harmful to the cadmium column and could severely affect the baseline. Therefore, 20 cm back pressure tubing was connected to the outlet of the LWCC, and stop-flow was recommended while changing samples in order to avoid bubbles.

3. Results and discussion

3.1. Reagent mixture and injection strategies

During nitrate detection, the NH_4Cl buffer is usually used to buffer the sample solution at an appropriate pH to lower the risk of nitrate overreduction and reach nearly 100% nitrate reduction efficiency, even though theoretically NH_4Cl buffer is not necessary in nitrite detection. Therefore NH_4Cl buffer was applied in nitrite+nitrate detection in the proposed design; it was also used in the nitrite analytical channel of the design. There were mainly two reasons for this: first, by using the same buffer solution, even when switching between the two analytical channels the matrix would be matched; hence the Schlieren effect would be overcome. Secondly, NH_4Cl buffer would cover the variation of salinity and pH among standard solutions in the Milli-Q water and seawater sample thus minimize the matrix effect for nitrite detection, which will be discussed later in this paper.

There were two modes of reagent mixing in the rFIA manifold. The reagent could be directly mixed with the sample flow with peristaltic pump 2 (PP2) through a Y-shaped connector. While the reagent could first flow through the reagent loop, it would then be injected into the sample flow by switching the 6-port, 2-position valve 2 (V2). Since there were two chromogenic reagents (SAM and NED), three strategies of reagent mixing mode and adding order, as shown in Table 1, were investigated. Strategy no. 3 was finally selected because it had higher sensitivity and better peak shape.

3.2. Optimization of flow rate, reagent loop and mixing coils

The effect of various parameters, including lengths of the reagent loop and mixing coils, flow rates, and concentrations of the reagents, was investigated and optimized based on a univariate experimental design. For optimization of these parameters, a blank and a 25.0 nmol L^{-1} nitrate standard solution were used as testing samples. The sensitivity, sample throughput, and the peak shape were taken into consideration to evaluate the optimum parameters for the proposed method.

Table 1
Strategies of reagent mixing mode and adding order.

Test no.	Reagent mixing mode	
	Directly mixed with PP2	Injected by switching V2
1		SAM+NED
2	NED	SAM
3	SAM	NED

The effect of sample flow rate was tested in the range 0.50–1.25 mL min^{-1}. A sample flow rate of 0.67 mL min^{-1} was selected to maintain a proper sensitivity and a higher sample throughput. The flow rates of the buffer, SAM and NED were also optimized, as shown in Fig. 1.

The influence of the length of reagent loop, which represented the injected volume of NED, was investigated in the range 15–35 cm, while the sample flow rate was kept at 0.67 mL min^{-1}. The results showed that, if the reagent loop was longer than 30 cm, a double peak would appear, suggesting that the NED solution was not completely mixed with the sample. In consideration of the peak shape and sensitivity, a reagent loop of 20 cm with 160 μL injection volume was selected for the subsequent experiments.

In MC1, the sample–buffer and SAM were mixed, and in MC2, the sample–buffer–SAM and NED were mixed together for azo compound formation. The influences of the lengths of MC1 and MC2 were investigated. When MC1 was longer than 10 cm, the sensitivity was not improved with increasing length, but dispersion was higher; hence 10 cm was selected as optimum MC1 length. Increasing MC2 length from 50 cm to 250 cm showed no significant improvement on signal intensity; however MC2 length shorter than 100 cm caused a severe peak tailing. Balancing peak shape and analysis time, 200 cm tubing was selected to make the knotted reactor MC2.

3.3. Optimization of the chemical variables

Different concentrations of SAM, HCl and NED in reagent solutions were investigated within the range 0.5–4.0 g L^{-1}, 2–10% (v/v) and 0.05–0.25 g L^{-1}, respectively. SAM solution containing 1.5 g L^{-1} SAM and 4% (v/v) HCl, and 0.15 g L^{-1} NED solution were selected for higher sensitivity and lower blank value.

Based on a previous study [6], the concentration of NH_4Cl in the buffer solution was 10 g L^{-1} without further optimization. Effects of buffer pH on both nitrite and nitrate detection were investigated by adjusting pH using different volumes of 50% (v/v) $NH_3 \cdot H_2O$ solution. The blank, a 25.0 nmol L^{-1} nitrite, and a 25.0 nmol L^{-1} nitrate standard solution were used as the testing samples, and the results including the net absorbance are shown as average value ± standard deviation ($n=3$) in Fig. 2. In the case of both nitrite and nitrate, increasing pH from 7.5 to 8.5, although some changes in sample and blank signal occurred, the net absorbance remained almost constant. In order to make the sample and blank signals more constant and comparable, a pH of 8.2 was used for further experimental work.

3.4. The matrix effect

Nitrate and nitrite standards prepared in three different matrices, including Milli-Q water, seawater (salinity ~35) and saltwater (35‰ NaCl), were utilized to investigate the matrix effect on the determination with the manifolds shown in Fig. 3. It was believed that Milli-Q water and saltwater were neutral, and seawater and saltwater shared the same ion strength. As shown in Fig. 3, manifolds A, B and C were mainly identical in flow procedure, but with different solution/reagent connection. In manifold A, Milli-Q water and the nitrite sample were merged and mixed with the color developing reagents to form the azo compound, and then detected in the LWCC. While in manifold B, NH_4Cl buffer and nitrite sample were merged and detected. The nitrate sample was merged with NH_4Cl buffer, then reduced to nitrite with cadmium and detected in manifold C. In each case, nitrite or nitrate working standard solutions in three different matrices in the concentration range 0–200.0 nmol L^{-1} were measured and calculated. The results are shown in Table 2. The correlation coefficient (R^2) of each working standard curve was higher than 0.999. The ratio of the slope of working standard curves prepared in one of three different matrices to the one prepared in Milli-Q water in the same manifold could be adopted to evaluate the matrix effect.

Theoretically, a high pH value would block the formation of azo compound and depress sensitivity [6]. However, in manifold A, the sensitivity (slope) for seawater with a higher pH value (pH~8) was approximately 5% higher than that for Milli-Q water, and equal to that for saltwater with its lower pH value (pH=7). This indicated that the pH depression effect on method sensitivity had been completely overwhelmed by the ion strength effect. In the conventional manual spectrophotometric method there is no salt effect on sensitivity since nitrite completely reacts with the reagents [6]. In the rFIA system, where the reaction usually does not need to be completed, ion strength might accelerate the reaction and increase method sensitivity.

For manifold B, no sensitivity difference among the three matrices was found, suggesting that variations due to ion strength in the three different matrices were covered by the buffer. In other words, the matrix effect was negligible. Therefore, although it is not necessary for conventional manual spectrophotometric nitrite analysis, NH_4Cl buffer was applied in the nitrite analytical channel in this study. In this way, variation among standard solutions in Milli-Q water and seawater samples could be suppressed, and matrix effect was minimized. Similar results are reported using LWCC combined SCFA [23].

In manifold C, nitrate was reduced to nitrite with cadmium. The components which flowed out of the column were similar with those in manifold B. While there was no significant sensitivity difference among the three matrices in manifold B, about a 5% increase of sensitivity in seawater and saltwater was caused by the cadmium reduction process. Since the pH had been buffered, ion strength was still the key factor affecting the reduction process.

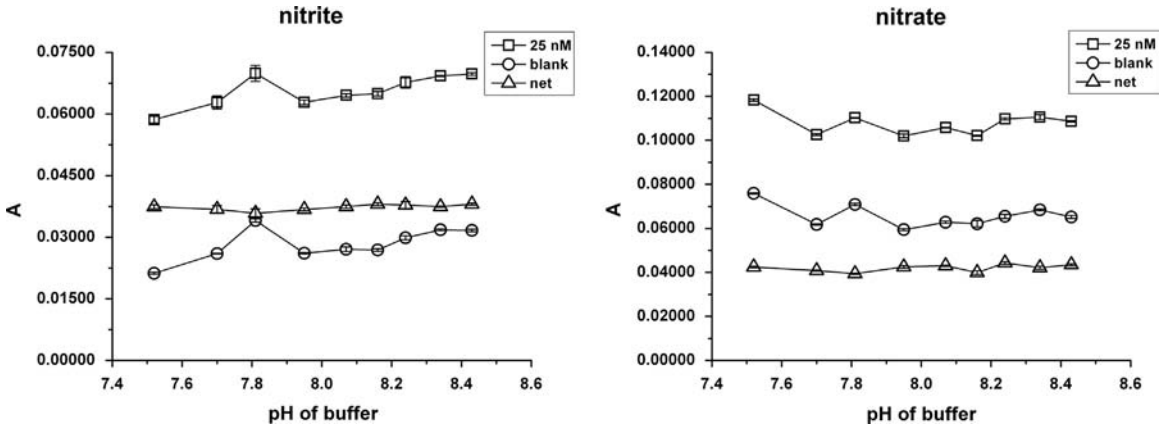

Fig. 2. Effects of NH_4Cl buffer pH on nitrite and nitrate detection signal. Error bars are ± S.D. ($n=3$).

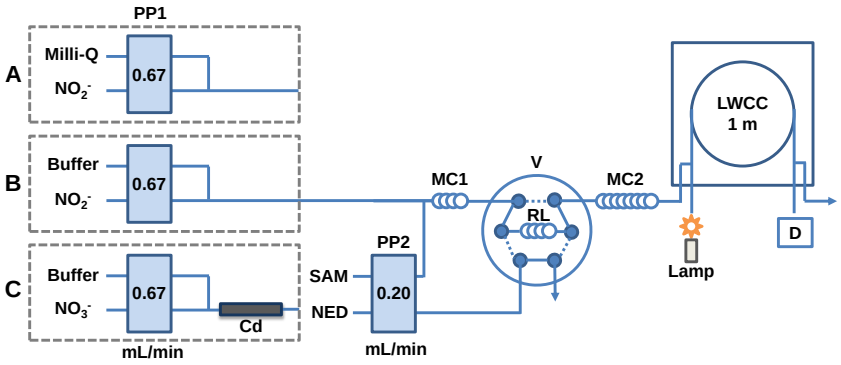

Fig. 3. Manifold utilized to investigate matrix effect.

Table 2
The calculated results of the working standard curves prepared in different matrices and measured with different manifolds.

Matrix	Manifold A		Manifold B		Manifold C	
	NO_2^- in Milli-Q water		NO_2^- in buffer		NO_3^- in buffer	
	Slope	Ratio[a] (%)	Slope	Ratio[a] (%)	Slope	Ratio[a] (%)
Milli-Q water	0.00146	–	0.00145	–	0.00149	–
Seawater	0.00153	104.8	0.00147	101.4	0.00156	104.7
Saltwater	0.00153	104.8	0.00145	100.0	0.00158	106.0

[a] Ratio: slope ratio of the curve with seawater or saltwater to the curve with Milli-Q water.

Table 3
Recovery of nitrite and nitrite+nitrate from seawater samples with the proposed method ($n=3$).

Sample no.	Nitrite				Nitrite+nitrate			
	Conc. (nmol L^{-1})	Added Conc. (nmol L^{-1})	Found Conc. (nmol L^{-1})	Recovery (%)	Conc. (nmol L^{-1})	Added Conc. (nmol L^{-1})	Found Conc. (nmol L^{-1})	Recovery (%)
1	5.1 ± 0.5	10.0	15.8 ± 0.7	107.2 ± 7.1	4.6 ± 0.2	5.0	9.4 ± 0.1	96.3 ± 2.4
2	5.8 ± 0.3	9.7	16.1 ± 0.3	105.6 ± 0.3	6.6 ± 0.1	5.0	11.3 ± 0.3	94.1 ± 5.4
3	7.5 ± 0.4	10.6	18.0 ± 0.3	99.1 ± 1.2	8.2 ± 0.1	5.0	13.5 ± 0.1	106.3 ± 2.5
4	7.6 ± 0.2	9.5	17.7 ± 0.6	105.7 ± 2.0	8.3 ± 0.1	5.0	13.8 ± 0.1	107.0 ± 1.2
5	8.3 ± 0.3	9.5	18.1 ± 0.2	103.0 ± 2.3	23.9 ± 0.1	20.5	45.1 ± 0.2	103.3 ± 1.2
6	9.0 ± 0.4	9.2	18.8 ± 0.2	105.1 ± 0.8	12.9 ± 0.1	10.0	22.8 ± 0.1	98.3 ± 1.0
7	10.3 ± 0.4	10.0	20.5 ± 0.2	101.9 ± 2.0	34.9 ± 0.2	20.0	55.2 ± 0.2	101.7 ± 1.1
8	10.9 ± 0.3	10.0	21.4 ± 0.3	104.5 ± 0.7	11.7 ± 0.1	9.7	21.1 ± 0.1	96.8 ± 0.4
9	20.0 ± 0.1	9.8	30.5 ± 0.2	107.5 ± 1.3	44.9 ± 0.1	20.5	65.8 ± 0.1	101.7 ± 0.6
10	43.2 ± 0.1	18.5	62.8 ± 0.1	106.0 ± 0.7	90.1 ± 0.3	20.5	112.0 ± 0.2	106.7 ± 1.0

In this study, reduction efficiency of the cadmium column remained almost near 100% in the three different matrices. It was supposed that the matrix effect observed was caused by the ion strength in seawater and saltwater dynamically affecting the reduction process. The specific chemical mechanism still needs further study. Repeat experimental correction or using low-nutrient seawater as a matrix for preparing the calibration standards would override the matrix effect.

3.5. Recovery

A recovery study was conducted to further evaluate the matrix effect. Nitrite and nitrate solutions with various concentrations were added into 10 seawater samples collected from the South China Sea to test the recovery. The recoveries for nitrite and nitrite+nitrate as shown in Table 3 were in the ranges 99.1–107.5% and 94.1–107.0%, presenting good accuracy and little matrix influence.

3.6. Analytical figures of merit

Under the optimized conditions, calibration curves for nitrite and nitrate were obtained over the concentration range 2–100 nmol L^{-1}. The regression equations were $A=0.00143\,C\ (NO_2^-)$ nmol $L^{-1}+0.03058$, with $R^2=0.99995$ ($n=7$), and $A=0.00155\,C\ (NO_3^-)$ nmol $L^{-1}+0.05995$, with $R^2=0.99965$ ($n=7$), where A was the absorbance and $C\ (NO_2^-)$ and $C\ (NO_3^-)$ were the concentrations of nitrite and nitrate, respectively. The upper linear limit of nitrite and nitrate could both be expanded to 500 nmol L^{-1} and might be further expanded by choosing a less sensitive detection wavelength. The method detection limit for nitrite and nitrate, estimated as three times the standard deviation of the blanks ($n=11$), was 0.6 nmol L^{-1}, which was low enough to determine the nitrite and nitrate concentration in open ocean. The sample throughput was five samples per hour, with both nitrite and nitrate analyzed in triplicate. Fig. 4 illustrates the typical output signal of a Milli-Q water sample

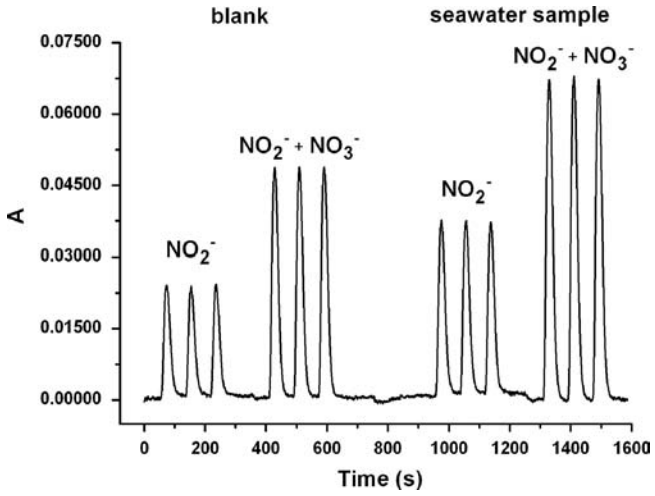

Fig. 4. Typical output signal of the blank and a seawater sample.

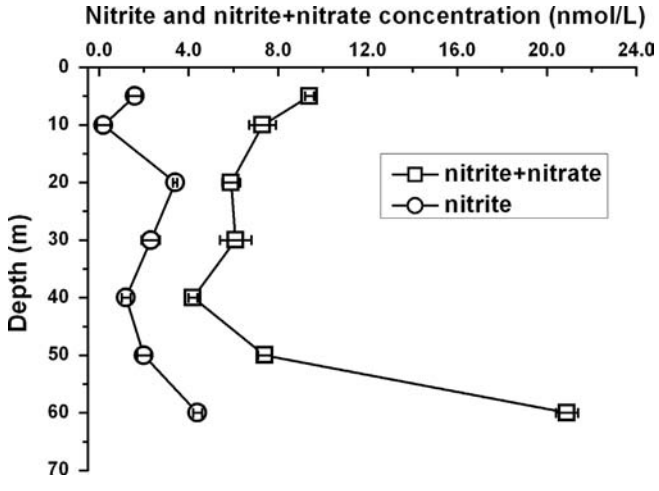

Fig. 6. Nitrite and nitrite+nitrate concentrations in surface water at station KK1 (18.2573°N, 115.6649°E) in the South China Sea in May 2011.

Table 4
Comparison of nitrite results of the proposed method and a reference method [22].

Sample no.	Conc. of nitrite ± SD (nmol L^{-1}) (n=3)		Calculated t-value	Critical t-value (P=0.95)
	Proposed method	Reference method		
1	14.6 ± 0.1	14.5 ± 0.1	1.10	2.78
2	27.4 ± 0.4	27.5 ± 0.2	0.26	2.78
3	113.0 ± 0.9	111.7 ± 0.1	2.56	2.78

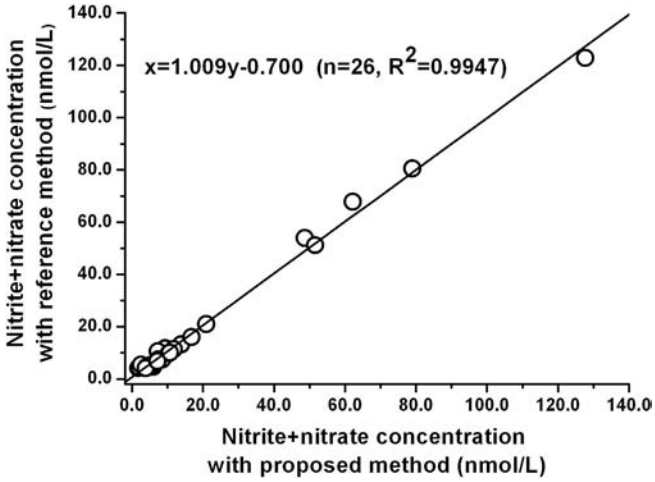

Fig. 5. Intercomparison data between the proposed method and a reference method [23].

as the blank and a seawater sample with 10.4 nmol L^{-1} nitrite and 14.1 nmol L^{-1} nitrite+nitrate.

The relative standard deviations (RSDs) for nitrite and nitrate at various concentrations in Milli-Q water and seawater were between 0.08 and 4.75%, showing good precision. During 10.5 h continuous measurement for 41 samples, the RSDs of transmission light strength of the baseline at detection wavelength 540 nm was 1.1%, suggesting little absorption onto the inner wall of the LWCC. Because, in rFIA, chromophore only exists in the injected reagent zone, the unreacted sample can behave as a washing solution to keep the LWCC clean. The total sample volume consumed for determination of nitrite and nitrite+nitrate was only 16 mL, which was acceptable for seawater analysis.

3.7. Comparison with reference methods

The intercomparison experiments were performed in order to further evaluate the accuracy of the method. In the intercomparison of nitrite results, three seawater samples were analyzed using the proposed method and an LWCC batch method developed by Yao et al. [22]. As the results shown in Table 4, the calculated t-values are less than the critical t-values, indicating no statistically significant difference between the two methods. The intercomparison of the nitrite+nitrate results was carried out between our rFIA–LWCC system and the results reported for an automated segmented flow analyzer (Bran+Luebbe AA3) combined with a 1.5 m LWCC system [23], and 26 seawater samples collected from the South China Sea were analyzed. As shown in Fig. 5, the results indicate good agreement between the two methods within a range 2–130 nmol L^{-1}.

3.8. Application

The method had been applied to the determination of nitrite and nitrite+nitrate in seawater samples collected from the South China Sea. A typical profile of station KK1 (18.2573°N, 115.6649°E) in the South China Sea in May 2011 is shown in Fig. 6, indicating the variations of nanomolar concentrations of nitrite and nitrate in the surface layer.

4. Conclusions

A simple rFIA method combined with a 1 m LWCC for simultaneous determination of nanomolar nitrite and nitrate in seawater was developed. The proposed method had the advantages of having low method detection limit, high precision and high sample throughput. There was no significant difference between the results obtained via the proposed and a reference method. The matrix effect was negligible. The proposed method could be applied to field and underway analysis of trace nitrite and nitrate and provide accurate, precise and real-time data for oceanography research.

Appendix A. Supplementary material

Supplementary data associated with this article can be found in the online version at http://dx.doi.org/10.1016/j.talanta.2013.09.042.

Acknowledgments

This work was financed by the Science Fund for Creative Research Groups of the National Natural Science Foundation of China (Grant no. 41121091). The authors would like to thank Dr. Jian Ma of the College of the Environment & Ecology, Xiamen University for helpful advice. We also thank Chuanjun Du of the College of the Environment & Ecology, Xiamen University for supplying the seawater samples. Prof. John Hodgkiss is thanked for polishing the English.

References

[1] P.G. Falkowski, R.T. Barber, V. Smetacek, Science 281 (1998) 200–206.
[2] J.A. Brandes, A.H. Devol, C. Deutsch, Chem. Rev. 107 (2007) 577–589.
[3] D.E. Canfield, A.N. Glazer, P.G. Falkowski, Science 330 (2010) 192–196.
[4] J.E. Dore, D.M. Karl, Deep Sea Res. Part II: Top. Stud. Oceanogr. 43 (1996) 385–402.
[5] L.R. Adornato, E.A. Kaltenbacher, D.R. Greenhow, R.H. Byrne, Environ. Sci. Technol. 41 (2007) 4045–4052.
[6] K. Grasshoff, M. Ehrhardt, K. Kremling, Methods of Seawater Analysis, 2nd edn. Verlag Chemie, Weinheim, Germany, 1983, pp. 139–150.
[7] K.S. Johnson, R.L. Petty, Limnol. Oceanogr. 28 (1983) 1260–1266.
[8] C. Garside, Mar. Chem. 11 (1982) 159–167.
[9] T. Aoki, S. Fukuda, Y. Hosoi, H. Mukai, Anal. Chim. Acta 349 (1997) 11–16.
[10] Y. Kanda, M. Taira, Anal. Sci. 19 (2003) 695–699.
[11] P. Mikuška, Z. Večeřa, Anal. Chim. Acta 495 (2003) 225–232.
[12] H.D. Axelrod, N.A. Engel, Anal. Chem. 47 (1975) 922–924.
[13] R.T. Masserini, K.A. Fanning, Mar. Chem. 68 (2000) 323–333.
[14] V. Nguyen, H. Neumeister, G. Subklew, Fresenius' J. Anal. Chem. 363 (1999) 783–788.
[15] J.Z. Zhang, Anal. Sci. 22 (2006) 57–60.
[16] M.J. Moorcroft, J. Davis, R.G. Compton, Talanta 54 (2001) 785–803.
[17] S.C. Pai, S.W. Chung, T.Y. Ho, Y.J. Tsau, Int. J. Environ. Anal. Chem. 62 (1996) 175–189.
[18] M. Miró, A. Cladera, J.M. Estela, V. Cerdà, Analyst 125 (2000) 943–948.
[19] G. Chen, D. Yuan, Y. Huang, M. Zhang, M. Bergman, Anal. Chim. Acta 620 (2008) 82–88.
[20] M. Zhang, D. Yuan, G. Chen, Q. Li, Z. Zhang, Y. Liang, Microchim. Acta 165 (2009) 427–435.
[21] M. Zhang, D. Yuan, Y. Huang, G. Chen, Z. Zhang, Acta Oceanol. Sin. 29 (2010) 100–107.
[22] W. Yao, R.H. Byrne, R.D. Waterbury, Environ. Sci. Technol. 32 (1998) 2646–2649.
[23] J.Z. Zhang, Deep Sea Res. Part I: Oceanogr. Res. Pap. 47 (2000) 1157–1171.
[24] E.T. Steimle, E.A. Kaltenbacher, R.H. Byrne, Mar. Chem. 77 (2002) 255–262.
[25] L. Adornato, E. Kaltenbacher, T. Villareal, R. Byrne, Deep Sea Res. Part I: Oceanogr. Res. Pap. 52 (2005) 543–551.
[26] H. Takiguchi, A. Tsubata, M. Miyata, T. Odake, H. Hotta, T. Umemura, K. Tsunoda, Anal. Sci. 22 (2006) 1017–1019.
[27] Q.P. Li, D.A. Hansell, J.Z. Zhang, Limnol. Oceanogr.: Methods 6 (2008) 319–326.
[28] M.D. Patey, M.J.A. Rijkenberg, P.J. Statham, M.C. Stinchcombe, E.P. Achterberg, M. Mowlem, TrAC Trends Anal. Chem. 27 (2008) 169–182.
[29] L.J. Gimbert, P.J. Worsfold, TrAC Trends Anal. Chem. 26 (2007) 914–930.
[30] R.N.M.J. Páscoa, I.V. Tóth, A.O.S.S. Rangel, Anal. Chim. Acta 739 (2012) 1–13.
[31] P.J. Worsfold, Microchim. Acta 154 (2006) 45–48.
[32] F.R. Mansour, N.D. Danielson, TrAC Trends Anal. Chem. 40 (2012) 1–14.
[33] J. Ma, D. Yuan, M. Zhang, Y. Liang, Talanta 78 (2009) 315–320.
[34] Y. Huang, D. Yuan, J. Ma, M. Zhang, G. Chen, Microchim. Acta 166 (2009) 221–228.
[35] J.Z. Zhang, C.J. Fischer, P.B. Ortner, Int. J. Environ. Anal. Chem. 76 (2000) 99–113.
[36] C. Infante, F.R.P. Rocha, Microchem. J. 90 (2008) 19–25.